THE JOURNAL OF PHYSICAL CHEMISTRY C

Article

pubs.acs.org/JPCC

Dependence of Exciton Diffusion Length on Crystalline Order in Conjugated Polymers

Myungsun Sim, Jisoo Shin, Chiyeoung Shim, Min Kim, Sae Byeok Jo, Joo-Hyun Kim, and Kilwon Cho*

Department of Chemical Engineering, Pohang University of Science and Technology, Pohang, 790−784, Korea

Supporting Information

ABSTRACT: Exciton diffusion in organic semiconductors is crucial to the performance of organic solar cells. Here, we measured the exciton diffusion length in poly(3-hexylthiophene) (P3HT) as a function of the crystalline order using spectrally resolved photoluminescence quenching (SR-PLQ) techniques. The crystalline order in the P3HT films, characterized according to the mean crystal size and normalized crystallinity, was varied by changes in thermal treatment temperatures. The exciton diffusion length increased from 3 to 7 nm as the mean crystal size increased more than twice and the crystallinity increased by a factor of 6. A higher crystalline order improved the spectral overlap and reduced the distance between chromophores, enhancing Förster-mediated exciton diffusion. The higher crystalline order also lengthened the conjugated segments and reduced the energetic disorder, producing favorable condition for exciton hopping.

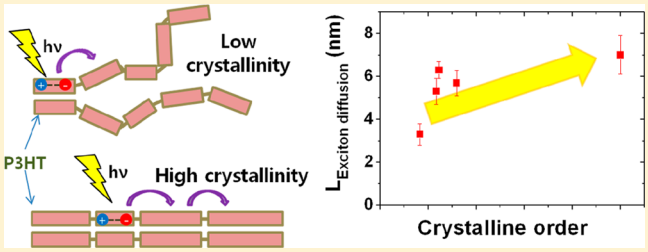

INTRODUCTION

In recent years, polymer solar cells have been extensively studied as low-cost alternative energy sources. The power conversion efficiency of a polymer solar cell exceeded 8%;[1] however, further increases are limited in part by the very short exciton diffusion lengths (L_D) in organic semiconductors. The exciton diffusion length in an organic semiconductor is typically much smaller than the optical absorption length. Extending the exciton diffusion length is an important consideration toward optimizing the design of polymer solar cells.[2−5]

Exciton diffusion in conjugated polymers has been less extensively studied than that in small molecules.[6−18] Small conjugated molecules are amenable to thickness-dependent photoluminescence (PL) quenching techniques used to measure the L_D values, because the film thickness may be tuned using evaporation deposition.[6,19] However, conjugated polymers are not suitable for this technique because polymer films are usually deposited by a solution process that is not amenable to the formation of continuous thin films several nanometers in thickness. Most of the studies on exciton diffusion length in organic semiconductors have focused on measurement methods rather than on the correlations between the material properties and the L_D values.[9,20−23] Recently, Lunt et al. reported the relationship between the crystalline order and the exciton diffusion length in small-molecule semiconductors.[24] However, this study is not directly applicable to conjugated polymer systems because exciton diffusion in a conjugated polymer differs from that in a small-molecule film.

Unlike the small-molecule semiconductors, conjugated polymers include a distribution of chromophore sizes.[25] A conjugated polymer chain consists of conformational subunits separated by conjugation breaks caused by twists or kinks in the backbone chain. A conformational subunit acts as an effective chromophore, that is, a light-absorbing unit, in which electronic excitation is localized after photoexcitation. The chromophore size distribution in a conjugated polymer film is affected by the crystalline order which can be easily controlled by varying the processing conditions, such as the coating process or the application of post-treatments.

Thermal treatments are widely used to enhance the performances of polymer optoelectronic devices. Thermally treated polymer semiconductors display greater crystalline orderings, which improves the light absorption and charge transport.[26−29] The size and spatial distributions of the chromophores can vary with the crystalline order. Such properties affect exciton diffusion because excitons migrate by hopping between chromophores.

Here, we investigated the effects of the crystalline order on the exciton diffusion lengths in poly(3-hexylthiophene) (P3HT) films. The degree of crystalline order in a P3HT film was controlled by thermal treatment. The exciton diffusion lengths were measured using a spectrally resolved photoluminescence quenching (SR-PLQ) method,[22] which had been modified for application to soluble polymer systems. The exciton diffusion lengths in P3HT increased with the crystalline domain size and crystallinity. A higher crystalline order improved the spectral overlap and reduced the distance between chromophores, enhancing Förster-mediated exciton diffusion. The higher crystalline order also lengthened the

Received: March 10, 2013
Revised: December 19, 2013
Published: December 23, 2013

   dx.doi.org/10.1021/jp409776s | J. Phys. Chem. C 2014, 118, 760−766

conjugated segments and reduced the energetic disorder, both of which improvements tended to favor exciton hopping.

EXPERIMENTAL SECTION

Regioregular P3HT (4002-E) samples were purchased from Rieke Metals Inc. Thick P3HT films were spin-coated in chloroform or chlorobenzene solvents in a glovebox under a nitrogen atmosphere. The film thickness was about 250 nm. The films were thermally treated, then cooled slowly. The crystalline order was determined by the thermal treatment temperature, which was varied over the range of 180−235 °C.

The crystalline orders of the as-cast and annealed films were characterized by grazing incidence X-ray diffraction (GIXD). The full width of half-maximum (fwhm) and *d*-spacing of the (100) diffraction peak were analyzed by one-dimensional (1D) GIXD experiments in both the out-of-plane and in-plane configurations, and the molecular orientations and angular integrated diffraction peaks were analyzed by two-dimensional (2D) GIXD experiments. The morphologies of the films were characterized by atomic force microscopy (AFM) (Digital Instruments Multimode) operated in the tapping mode.

SR-PLQ measurements were carried out in a spectrofluorometer (Jasco). The excitation spectra of the P3HT films containing poly(vinylpyrrolidone) (PVP) blocking or TiO_x quenching layers were collected over the range of λ = 400−600 nm at a peak emission wavelength of 650 nm. The thicknesses of the PVP and TiO_x layers were about 30 nm. An exciton blocking layer was found to be necessary to avoid exciton quenching at the free P3HT surface. The degree of PL quenching, η, was calculated as the ratio of the excitation spectrum intensity in the sample prepared with a blocking layer (PL_B) to the intensity in an equivalent sample prepared with a quenching layer (PL_Q). The excitation spectra were corrected for transmission losses and reflectance variations in the quenching and blocking layers, as measured using the spectrophotometers. The absorption coefficients were calculated by dividing the absorbance acquired using the spectrophotometer (Varian, CARY-5000) by the film thickness determined using an ellipsometer (M-200 V, H. A. Woollam Co., Inc.) and corroborated by AFM measurements. Modified absorption coefficients (α') were obtained by adjusting the absorption coefficients (α) for the incidence illumination angle (θ_λ): $\alpha' = \alpha/\cos\theta_\lambda$. The θ_λ was 60°. Energy transfer to the quenching layer was negligible because the TiO_x band gap was large; therefore, η was related to the L_D values extracted according to $\eta = \alpha' L_D + 1$.[22] The error bars on the diffusion length were propagated from the uncertainty in the PL measurements for each sample and from the error-weighted least-squares fitting.

RESULTS AND DISCUSSION

The extent of crystalline order in the P3HT films was varied according to thermal treatment temperatures and characterized by GIXD, as shown in Figure 1 and summarized in Table 1. The film thermally annealed at 235 °C formed a melt-crystallized film with the highest degree of crystallinity observed in this data set. The positions of (100) and (010) diffraction peaks of the films were slightly shifted so that the *d*-spacing of the (100) and (010) planes decreased slightly as the thermal treatment temperature increased. The intensity (brightness) of the diffraction image, corresponding to the (100), (200), and (300), and (010) peaks of the P3HT films, increased as the

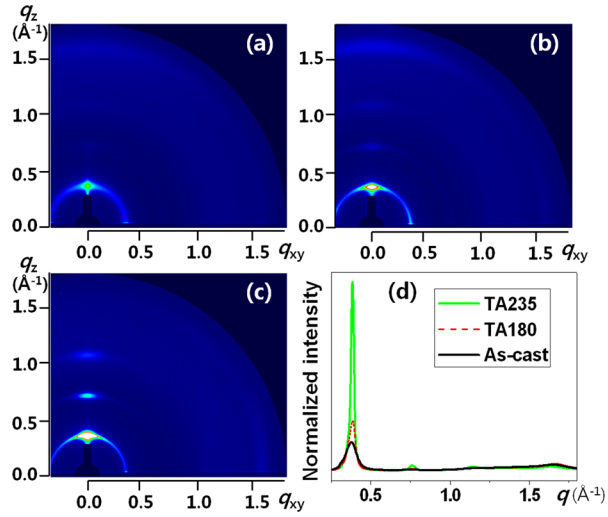

Figure 1. Two-dimensional GIXD patterns for (a) an as-cast P3HT film and thermally treated P3HT films at (b) 180 and (c) 235 °C. (d) Angular-integrated diffraction patterns of the films.

thermal treatment temperature increased. The relative degree of the P3HT crystallinity (N) was quantitatively determined as a function of the thermal treatment temperature by measuring the angular-integrated intensity of the (100) diffraction peak because the GIXD data showed the (100) diffraction peak was the most dominant peak compared to other diffraction peaks. The intensity of each film was then normalized by the intensity of the melt-crystallized film. This relative degree of crystallinity (N) increased with the thermal treatment temperature, suggesting that the P3HT chains became more mobile and shifted to positions that were more thermodynamically stable resulting in a larger number of crystallites. The N value of the melt-crystallized film was 6 times larger than that of the as-cast film.

The diffraction peaks narrowed as the thermal treatment temperature increased. The narrowing of the diffraction peaks indicated an increase in the coherent domain size which could be estimated using the Scherrer equation, given by

$$R = \frac{K\lambda}{\text{fwhm}\cos\theta} \quad (1)$$

where K is the dimensionless Scherrer constant, λ is the incident X-ray wavelength, fwhm is the full width at half-maximum of the peak, and θ is the Bragg angle. The stacking distances and coherent domain sizes of the (100) and (010) peaks for the thermally annealed samples are given in Table 1. The (100) and (010) coherent domain sizes increased with the thermal treatment temperature, suggesting that the stacking defects decreased and the intrachain/interchain ordering increased. The (100) coherent domain size of the melt-crystallized film was more than twice larger than that of the as-cast film. Instrumental broadening effects were not considered here. The instrumental broadening was expected to remain constant and provide a negligible effect relative to the sample broadening.[30] This allowed the sample features to be compared directly.

The P3HT film surfaces were observed by AFM. Figure 2 shows that the morphological feature of the P3HT crystal became clearer and the P3HT crystal domain size seemed to increase as the thermal treatment temperature increased. P3HT films are polycrystalline films containing randomly oriented

dx.doi.org/10.1021/jp409776s | J. Phys. Chem. C 2014, 118, 760−766

Table 1. Lattice Constants, Mean Crystal Sizes, Normalized Angular-Integrated Intensities, and Exciton Diffusion Lengths for the P3HT Crystallites in As-Cast and Thermally Treated Films

thermal treatment temperature [°C]	lattice constant [nm]			coherent domain size [nm]			normalized angular-integrated intensity (N)	exciton diffusion length [nm]
	$(100)_v$	$(100)_h$	$(010)_h$	$(100)_v$	$(100)_h$	$(010)_h$	(100) for each film (100) for the melt-crystallized film	
as-cast	1.65	1.69	0.39	9.8	14.2	-	0.15	3.3
180	1.62	1.68	0.39	14.7	25.1	6.3	0.26	5.8
235	1.61	1.68	0.38	31.6	34.2	7.7	1.00	7

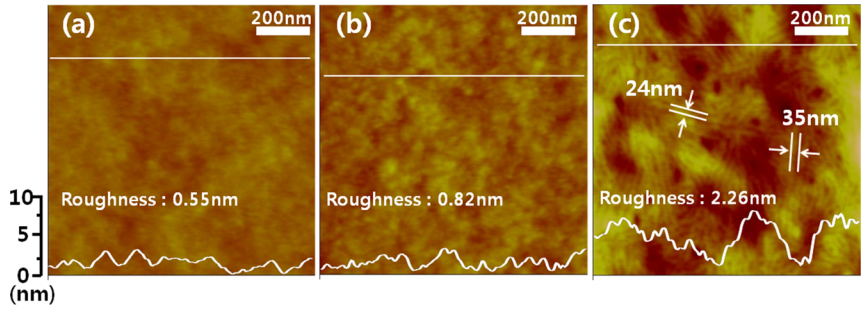

Figure 2. AFM images and height profiles of (a) an as-cast P3HT film and thermally treated P3HT films at (b) 180 and (c) 235 °C.

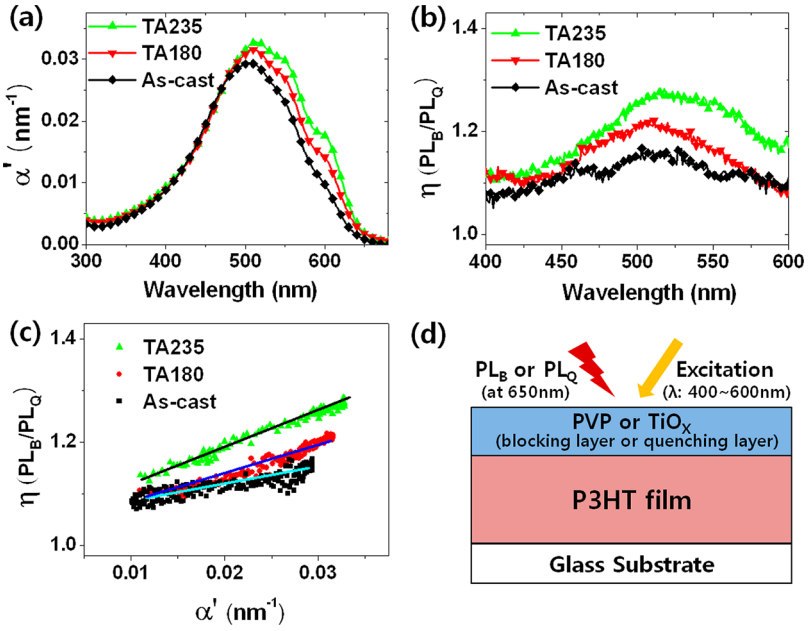

Figure 3. Measurement of P3HT diffusion length using spectrally resolved photoluminescence quenching. (a) Modified absorption coefficients for the non-normal incidence (α'), (b) the degree of luminescence quenching (η) vs wavelength, and (c) η vs α' for the as-cast (■) and thermally treated films at 180 (●) and 235 °C (▲). (d) Schematic diagram of the sample structures and measurement system used for the exciton diffusion analysis.

crystal domains. The melt-crystallized P3HT film prepared at 235 °C displayed a nanofibrillar structures with a width of 20–40 nm and a length of several micrometers (Figure 2c). The width and length of the P3HT nanofiber are related to the crystal domain sizes along the (001) and (010) directions, respectively.[31] The (001) and (010) crystal domain sizes of the melt-crystallized film were dramatically increased, compared to those of as-cast film. As shown in Figure 2c, the real (010) crystal domain size of the melt-crystallized film could be much larger than the coherent domain size obtained by GIXD (Table 1) because the coherent domain sizes were estimated using the Scherrer equation based on a spherical shape crystal which is not accurate for a fibrillar crystal. Furthermore, the (010) diffraction peak was observed in the high-angle region where the diffraction peak has a relatively low resolution due to geometric effects, compared to the diffraction peak in the low-angle region. However, as deduced from AFM and GIXD results, it is clear that the crystal size in the P3HT film increased in all directions as the thermal treatment temperature increased.

The exciton diffusion lengths were measured as a function of the thermal treatment temperature (which modulated the extent of crystalline order) using the SR-PLQ technique,[22] as shown in Figure 3. The degree of PL quenching (η) varies linearly with the modified absorption coefficient with incident illumination angle (θ_λ): $\eta = (\alpha/\cos\theta_\lambda)L_D + 1 = \alpha' L_D + 1$,

dx.doi.org/10.1021/jp409776s | J. Phys. Chem. C 2014, 118, 760–766

which was obtained by solving the one-dimensional steady-state exciton diffusion equation for the thick P3HT film.[22] As shown in Figure 3c, the slope of a plot of η versus α' then yields the exciton diffusion length, L_D. As the thermal treatment temperature increased, both the α' value and the η value increased (Figure 3, parts a and b); however, the α' value increased to a lesser degree than the η value. As a result, the exciton diffusion length increased as the thermal treatment temperature increased (Figure 3c).

As shown in Table 1, the exciton diffusion length increased as the crystalline order increased. The exciton diffusion length increased from 3 to 7 nm as the mean crystal size in the case of a simple cubic P3HT crystal increased more than twice, and the relative degree of crystallinity increased by a factor of 6. Figure 4 shows the relationship between exciton diffusion length and

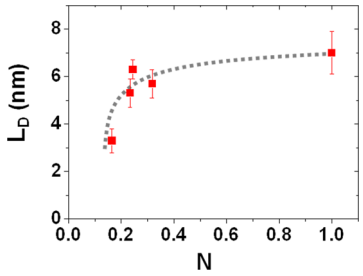

Figure 4. Exciton diffusion length vs the relative degree of crystallinity (N) for the P3HT film.

the relative degree of crystallinity (N). The exciton diffusion length increased dramatically at the low crystalline order and became saturated at the high crystalline order.

The diffusion length trends in P3HT were further explored by considering line dipole approximation and the weak dipole−dipole coupling limit, in which strong exciton−phonon interactions produce random exciton hopping behaviors.[32] In this case, line dipole Förster-type energy transfer rate was used to describe singlet exciton hopping via[33,34]

$$k_{DA} = \left(\frac{2\pi}{\hbar}\right) V_{DA}{}^2 J \approx \frac{\Phi_F}{\tau_D n^4} \left(\sum_{k,l}^{N} \Psi_k |\Gamma_{kl}| r_{DA}{}^{-3} \Psi_l\right)^2 J \quad (2)$$

and

$$V_{DA} \propto \frac{1}{r_{DA}} \quad (3)$$

where V_{DA} is the electronic coupling between the donor and acceptor chromophores, Γ is the dipole orientation factor, n is the refractive index, J is the spectral overlap integral between the emission spectrum of the donor chromophore and the absorption spectrum of the acceptor chromophore, Φ_F is the fluorescence yield, r_{DA} is the average hopping distance between a donor chromophore and an acceptor chromophore, and τ_D is the fluorescence lifetime of the donor chromophore.

To get more insights of exciton diffusion lengths, we have discussed the effects of each parameter on the L_D in eq 2. The dipole factor for a crystalline material is $\Gamma = \cos(\theta_{AD}) - 3\cos(\theta_A)\cos(\theta_D)$, where θ_{AD} is the angle between the donor and acceptor dipole moments and θ_A and θ_D are the angles between the molecular stacking direction and the dipole moment of the donor (D) and acceptor (A) chromophore pairs.[22] We assumed that Γ changed negligibly with the crystalline ordering because of random polymer conformations and spatial distributions of chromophores. The value of n in a P3HT film was not expected to change much with the degree of crystalline order because n is a material property of the material itself.

The fluorescence yield, Φ_F, is the ratio between the number of photons emitted through fluorescence and the number of photons absorbed by a chromophore. In case of large grains in molecular organic semiconductors, the number of photons emitted through fluorescence increases by reducing non-radiative exciton loss at grain boundaries. The fluorescence quantum yield of 3,4,9,10-perylenetetracarboxylic dianhydride, a polycrystalline small molecule, was previously found to increase with the grain sizes.[24] Unlike small-molecule semiconductors, the chromophore size (effective conjugation length) in a polymer chain can be enlarged by thermal treatments, which results in an increase of the transition dipole moments of the chromophores and thus the enhancement of the absorption coefficients.[32] As shown Figure 3a, thermal treatments of a P3HT film increased the absorption coefficient of P3HT and thus the number of photons absorbed by the P3HT film. The fluorescence quantum yield, Φ_F, was not expected to vary with the degree of crystalline order in the P3HT films (Table T1 in the Supporting Information).

The spectral overlap integral, J, quantifies the overlap between the normalized donor fluorescence and acceptor absorption spectra,[35,36] according to

$$J = \int F_D(\lambda) A_A(\lambda) \lambda^4 \, d\lambda \quad (4)$$

J could not be obtained from the thick P3HT films studied here because the chromophores in the P3HT films were characterized by a size distribution. It was experimentally impossible to obtain the fluorescence and absorption spectra of each chromophore and calculate J exactly for each chromophore; however, the J values for each P3HT film could be qualitatively estimated based on a film's static fluorescence and absorption spectral overlap integrals. The static spectrum of a film is the sum of the spectra of each chromophore in the film. Figure 5 shows the normalized absorption and fluorescence

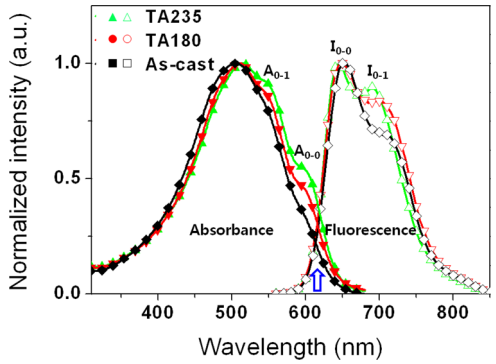

Figure 5. Normalized absorption (left) and fluorescence (right) spectra of the as-cast (■ and □) and thermally treated P3HT films at 180 (● and ○) and 235 °C (▲and △).

spectra for as-cast and thermally annealed P3HT films. An increase in the coherent domain size and relative degree of crystallinity in the conjugated polymers was correlated with a decrease in the number of defect sites and an increase in the intra/interchain order. High intra/interchain order indicated that the chains within each aggregate domain assumed a more rigid and planar form.[37] Therefore, the main absorption peaks

dx.doi.org/10.1021/jp409776s | J. Phys. Chem. C 2014, 118, 760−766

for the P3HT films were red-shifted from 505 to 514 nm, and the shoulder peaks at around 550 and 600 nm became more pronounced as the thermal treatment temperature increased. The fluorescence spectrum became slightly blue-shifted as the thermal treatment temperature increased because the high intra/interchain order hinders the torsional relaxation in the excited conjugated segments prior to fluorescence.[25,38,39] As a result, the overlap integral between the fluorescence and absorption spectra increased as the degree of crystalline order increased. This result suggested that J between the chromophore increased on average as the degree of crystalline order increased. This larger spectral overlap integral increased the Förster radius, R_0, and promoted exciton migration.

As the degree of crystalline order increased, the P3HT chain packing became more compact, as shown in Table 1. The lattice constants for the (100) and (010) planes decreased slightly as the thermal treatment temperature increased, and the P3HT film thickness decreased slightly. These results indicated that the P3HT chain packing density increased, bringing the chromophores closer to one another. As shown in eqs 2 and 3, the exciton diffusion length depends on the average hopping distance, r_{DA}, according to an inverse second power law. Exciton diffusion may, therefore, be enhanced in thermally treated films characterized by a high chain packing density. These results were consistent with the experimentally observed increase in exciton migration in going from a solution to a solid state due to the emergence of channels that promote hopping between chains in close contact.[32,40]

An increase in the average effective conjugation length with the thermal treatment temperature also enhanced exciton diffusion. The conjugation length of a polymer is closely related to the exciton bandwidth (W) induced by interchain interaction. The exciton bandwidth decreases as the conjugation length increases when the conjugation length is longer than the intermolecular separation according to quantum chemical calculations.[41,42] The exciton bandwidth can be quantitatively estimated form the ratio of the 0−0 transition and 0−1 transition peaks in the absorption spectrum (Figure 5) according to the following expression:[42−44]

$$\frac{A_{0-0}}{A_{0-1}} \approx \frac{(1 - 0.24W/\omega_0)^2}{(1 + 0.073W/\omega_0)^2} \quad (5)$$

where ω_0 is the intramolecular vibration frequency. Equation 5 shows that a lower exciton bandwidth is expected for a higher ratio between the intensity of the 0−0 transition (A_{0-0}) and that of the 0−1 transition (A_{0-1}). The values of A_{0-0} and A_{0-1} were obtained from fits to the absorption spectrum (Figure S2 in the Supporting Information). Table 2 reveals that the values of exciton bandwidth W/ω_0 decreased as the thermal treatment temperature increased. This suggested that the average effective conjugation length (chromophore size) in the polymer chains increased with the thermal treatment temperature. Thermally activated exciton hopping between large chromophores can be more effective than that between small chromophores because it requires the fewer number of hops.[45,46] Therefore, larger chromophores can enhance the exciton diffusion length.

Energetic disorder can reduce the exciton diffusion length.[47,48] Variations in the molecular conformation or size of conjugated segments (especially in conjugated polymers), inhomogeneities in the intermolecular interactions, chemical defects, or impurities lead to a Gaussian distribution of the HOMO−LUMO energy gaps—and the excitonic energies. Excitons undergo random walk migration (diffusion) among energy sites (conjugated segments) via energy transfer. The half-width σ of the Gaussian distribution of the energy sites is a measure of the site energy disorder, and the exciton diffusion length can increase as σ decreases. We estimated the half-widths σ from the exciton bandwidth W and the ratio (I_{0-0}/I_{0-1}) of the 0−0 to 0−1 emission peaks (Figure 5 and Figure S3 in the Supporting Information) using a simplified expression of Spano's model:[42,43]

$$\frac{I_{0-0}}{I_{0-1}} \approx \frac{(1 - 0.24W/\omega_0)^2}{2e^{-2}(1 - 0.39W/\omega_0)^2}\frac{\sigma^2}{W^2} \quad (6)$$

This expression is expected to be valid under conditions of spatially uncorrelated disorder, with a Huang−Rhys factor of $\lambda^2 = 1$. Equation 6 suggests that a lower exciton bandwidth and/or higher disorder are expected if 0−0 emission bands are more intense than the 0−1 emission bands. As shown in Table 2, the disorder (σ/ω_0) decreased as the thermal treatment temperature increased, suggesting that the thermal-treatment-induced crystalline order reduced site energy disorder, thereby increasing the exciton diffusion length.

Table 2. The 0-0 to 0-1 Peak Intensity Ratio from the Absorption and Emission Spectra, the Exciton Band Widths (W/ω_0), and the Disorder Parameters (σ/ω_0) for the As-Cast and Thermally Treated P3HT Films

thermal treatment temperature [°C]	A_{0-0}/A_{0-1}	I_{0-0}/I_{0-1}	W/ω_0	σ/ω_0
as-cast	0.424	1 450	1.123	0.319
180	0.529	1.195	0.931	0.1 88
235	0.592	1.121	0.778	0.135

CONCLUSIONS

We investigated the effects of crystalline order on the exciton diffusion length in a P3HT film. The crystalline order of a P3HT film was determined based on the mean crystal size and the normalized crystallinity, which increased with thermal treatment temperature. The exciton diffusion length was measured using a modified SR-PLQ method. The exciton diffusion length increased from 3 to 7 nm as the mean crystal size increased more than twice, and the crystallinity increased by a factor of 6. The increase in P3HT crystalline order improved the spectral overlap integral between the donor fluorescence and acceptor absorption and brought the chromophores closer to one another, thereby enhancing Förster-mediated exciton diffusion. The higher crystalline order favored the formation of longer conjugated segments and reduced the energetic disorder, producing favorable condition for exciton hopping. In summary, a higher crystalline order improved the exciton diffusion length in P3HT films. This result will contribute to the understanding of exciton diffusion in polymer solar cells.

ASSOCIATED CONTENT

Supporting Information

Rocking-curve on the (100) diffraction peak, fluorescence quantum yield, and analysis of absorption and fluorescence spectra. This material is available free of charge via the Internet at http://pubs.acs.org.

dx.doi.org/10.1021/jp409776s | J. Phys. Chem. C 2014, 118, 760−766

AUTHOR INFORMATION

Corresponding Author

*E-mail: kwcho@postech.ac.kr.

Notes

The authors declare no competing financial interest.

ACKNOWLEDGMENTS

This work was supported by a grant (code no. 2011-0031628) from the Center for Advanced Soft Electronics under the Global Frontier Research Program of the Ministry of Science, ICT and Future Planning, Korea. The authors thank the Pohang Accelerator Laboratory for providing the synchrotron radiation sources at 1D, 3C, 9A, and 9C beam lines used in this study.

REFERENCES

(1) Dou, L. T.; You, J. B.; Yang, J.; Chen, C. C.; He, Y. J.; Murase, S.; Moriarty, T.; Emery, K.; Li, G.; Yang, Y. Tandem polymer solar cells featuring a spectrally matched low-bandgap polymer. *Nat. Photonics* **2012**, *6*, 180−185.

(2) Kannan, B.; Castelino, K.; Majumdar, A. Design of nanostructured heterojunction polymer photovoltaic devices. *Nano Lett.* **2003**, *3*, 1729−1733.

(3) Heremans, P.; Cheyns, D.; Rand, B. P. Strategies for Increasing the Efficiency of Heterojunction Organic Solar Cells: Material Selection and Device Architecture. *Acc. Chem. Res.* **2009**, *42*, 1740−1747.

(4) Kim, J. S.; Park, Y.; Lee, D. Y.; Lee, J. H.; Park, J. H.; Kim, J. K.; Cho, K. Poly(3-hexylthiophene) Nanorods with Aligned Chain Orientation for Organic Photovoltaics. *Adv. Funct. Mater.* **2010**, *20*, 540−545.

(5) Currie, M. J.; Mapel, J. K.; Heidel, T. D.; Goffri, S.; Baldo, M. A. High-efficiency organic solar concentrators for photovoltaics. *Science* **2008**, *321*, 226−228.

(6) Peumans, P.; Yakimov, A.; Forrest, S. R. Small molecular weight organic thin-film photodetectors and solar cells. *J. Appl. Phys.* **2003**, *93*, 3693−3723.

(7) Shaw, P. E.; Ruseckas, A.; Samuel, I. D. W. Exciton diffusion measurements in poly(3-hexylthiophene). *Adv. Mater.* **2008**, *20*, 3516−3520.

(8) Scully, S. R.; McGehee, M. D. Effects of optical interference and energy transfer on exciton diffusion length measurements in organic semiconductors. *J. Appl. Phys.* **2006**, *100*, 034907.

(9) Markov, D. E.; Amsterdam, E.; Blom, P. W. M.; Sieval, A. B.; Hummelen, J. C. Accurate measurement of the exciton diffusion length in a conjugated polymer using a heterostructure with a side-chain cross-linked fullerene layer. *J. Phys. Chem. A* **2005**, *109*, 5266−5274.

(10) Zhou, Y. C.; Wu, Y.; Ma, L. L.; Zhou, J.; Ding, X. M.; Hou, X. Y. Exciton migration in organic thin films. *J. Appl. Phys.* **2006**, *100*, 023712.

(11) Rim, S. B.; Fink, R. F.; Schoneboom, J. C.; Erk, P.; Peumans, P. Effect of molecular packing on the exciton diffusion length in organic solar cells. *Appl. Phys. Lett.* **2007**, *91*, 173504.

(12) Kurrle, D.; Pflaum, J. Exciton diffusion length in the organic semiconductor diindenoperylene. *Appl. Phys. Lett.* **2008**, *92*, 133306.

(13) Luhman, W. A.; Holmes, R. J. Investigation of Energy Transfer in Organic Photovoltaic Cells and Impact on Exciton Diffusion Length Measurements. *Adv. Funct. Mater.* **2011**, *21*, 764−771.

(14) Marciniak, H.; Li, X. Q.; Wurthner, F.; Lochbrunner, S. One-Dimensional Exciton Diffusion in Perylene Bisimide Aggregates. *J. Phys. Chem. A* **2011**, *115*, 648−654.

(15) Dimitrov, S. D.; Nielsen, C. B.; Shoaee, S.; Tuladhar, P. S.; Du, J. P.; McCulloch, I.; Durrant, J. R. Efficient Charge Photogeneration by the Dissociation of PC70BM Excitons in Polymer/Fullerene Solar Cells. *J. Phys. Chem. Lett.* **2012**, *3*, 140−144.

(16) Wiesenhofer, H.; Beljonne, D.; Scholes, G. D.; Hennebicq, E.; Bredas, J. L.; Zojer, E. Limitations of the Forster description of singlet exciton migration: The illustrative example of energy transfer to ketonic defects in ladder-type poly(para-phenylenes). *Adv. Funct. Mater.* **2005**, *15*, 155−160.

(17) Bredas, J. L.; Beljonne, D.; Coropceanu, V.; Cornil, J. Charge-transfer and energy-transfer processes in pi-conjugated oligomers and polymers: A molecular picture. *Chem. Rev.* **2004**, *104*, 4971−5003.

(18) Chen, L. C.; Roman, L. S.; Johansson, D. M.; Svensson, M.; Andersson, M. R.; Janssen, R. A. J.; Inganas, O. Excitation transfer in polymer photodiodes for enhanced quantum efficiency. *Adv. Mater.* **2000**, *12*, 1110−1114.

(19) Haugeneder, A.; Neges, M.; Kallinger, C.; Spirkl, W.; Lemmer, U.; Feldmann, J.; Scherf, U.; Harth, E.; Gugel, A.; Mullen, K. Exciton diffusion and dissociation in conjugated polymer fullerene blends and heterostructures. *Phys. Rev. B* **1999**, *59*, 15346−15351.

(20) Banerjee, S.; Parhi, A. P.; Iyer, S. S. K.; Kumar, S. Method of determining the exciton diffusion length using optical interference effect in Schottky diode. *Appl. Phys. Lett.* **2009**, *94*, 223303.

(21) Gommans, H.; Schols, S.; Kadashchuk, A.; Heremans, P.; Meskers, S. C. J. Exciton Diffusion Length and Lifetime in Subphthalocyanine Films. *J. Phys. Chem. C* **2009**, *113*, 2974−2979.

(22) Lunt, R. R.; Giebink, N. C.; Belak, A. A.; Benziger, J. B.; Forrest, S. R. Exciton diffusion lengths of organic semiconductor thin films measured by spectrally resolved photoluminescence quenching. *J. Appl. Phys.* **2009**, *105*, 053711.

(23) Ariu, M.; Sims, M.; Rahn, M. D.; Hill, J.; Fox, A. M.; Lidzey, D. G.; Oda, M.; Cabanillas-Gonzalez, J.; Bradley, D. D. C. Exciton migration in beta-phase poly(9,9-dioctylfluorene). *Phys. Rev. B* **2003**, *67*, 195333.

(24) Lunt, R. R.; Benziger, J. B.; Forrest, S. R. Relationship between Crystalline Order and Exciton Diffusion Length in Molecular Organic Semiconductors. *Adv. Mater.* **2010**, *22*, 1233−1236.

(25) Hwang, I.; Scholes, G. D. Electronic Energy Transfer and Quantum-Coherence in pi-Conjugated Polymers. *Chem. Mater.* **2011**, *23*, 610−620.

(26) Kim, J. S.; Lee, J. H.; Park, J. H.; Shim, C.; Sim, M.; Cho, K. High-Efficiency Organic Solar Cells Based on Preformed Poly(3-hexylthiophene) Nanowires. *Adv. Funct. Mater.* **2011**, *21*, 480−486.

(27) Savenije, T. J.; Kroeze, J. E.; Yang, X. N.; Loos, J. The effect of thermal treatment on the morphology and charge carrier dynamics in a polythiophene-fullerene bulk heterojunction. *Adv. Funct. Mater.* **2005**, *15*, 1260−1266.

(28) Erb, T.; Zhokhavets, U.; Gobsch, G.; Raleva, S.; Stuhn, B.; Schilinsky, P.; Waldauf, C.; Brabec, C. J. Correlation between structural and optical properties of composite polymer/fullerene films for organic solar cells. *Adv. Funct. Mater.* **2005**, *15*, 1193−1196.

(29) Kim, J. H.; Park, J. H.; Lee, J. H.; Kim, J. S.; Sim, M.; Shim, C.; Cho, K. Bulk heterojunction solar cells based on preformed polythiophene nanowires via solubility-induced crystallization. *J. Mater. Chem.* **2010**, *20*, 7398−7405.

(30) Roehling, J. D.; Arslan, I.; Moule, A. J. Controlling microstructure in poly(3-hexylthiophene) nanofibers. *J. Mater. Chem.* **2012**, *22*, 2498−2506.

(31) Ihn, K. J.; Moulton, J.; Smith, P. Whiskers of Poly (3-alkylthiophene)s. *J. Polym. Sci., Part B: Polym. Phys.* **1993**, *31*, 735−742.

(32) Hennebicq, E.; Pourtois, G.; Scholes, G. D.; Herz, L. M.; Russell, D. M.; Silva, C.; Setayesh, S.; Grimsdale, A. C.; Mullen, K.; Bredas, J. L.; Beljonne, D.; et al. Exciton migration in rigid-rod conjugated polymers: An improved Forster model. *J. Am. Chem. Soc.* **2005**, *127*, 4744−4762.

(33) Barford, W. Exciton transfer integrals between polymer chains. *J. Chem. Phys.* **2007**, *126*, 134905.

(34) Barford, W.; Bittner, E. R.; Ward, A. Exciton Dynamics in Disordered Poly(*p*-phenylenevinylene). 2. Exciton Diffusion. *J. Phys. Chem. A* **2012**, *116*, 10319−10327.

(35) Laquai, F.; Park, Y. S.; Kim, J. J.; Basche, T. Excitation Energy Transfer in Organic Materials: From Fundamentals to Optoelectronic Devices. *Macromol. Rapid Commun.* **2009**, *30*, 1203−1231.

(36) Beckers, E. H. A.; van Hal, P. A.; Schenning, A. P. H. J.; Elghayoury, A.; Peeters, E.; Rispens, M. T.; Hummelen, J. C.; Meijer, E. W.; Janssen, R. A. J. Singlet-energy transfer in quadruple hydrogen-bonded oligo(*p*-phenylenevinylene)-fullerene dyads. *J. Mater. Chem.* **2002**, *12*, 2054−2060.
(37) Ko, S. W.; Hoke, E. T.; Pandey, L.; Hong, S. H.; Mondal, R.; Risko, C.; Yi, Y. P.; Noriega, R.; McGehee, M. D.; Bredas, J. L.; Salleo, A.; Bao, Z. A.; et al. Controlled Conjugated Backbone Twisting for an Increased Open-Circuit Voltage while Having a High Short-Circuit Current in Poly(hexylthiophene) Derivatives. *J. Am. Chem. Soc.* **2012**, *134*, 5222−5232.
(38) Bai Xu, S. H. Molecular Control of Luminescence from Poly(3-hexy1thiophenes). *Macromolecules* **1993**, *26*, 4457−4460.
(39) Frolov, S. V.; Bao, Z.; Wohlgenannt, M.; Vardeny, Z. V. Excited-state relaxation in pi-conjugated polymers. *Phys. Rev. B* **2002**, *65*, 205209.
(40) Beljonne, D.; Pourtois, G.; Silva, C.; Hennebicq, E.; Herz, L. M.; Friend, R. H.; Scholes, G. D.; Setayesh, S.; Mullen, K.; Bredas, J. L. Interchain vs. intrachain energy transfer in acceptor-capped conjugated polymers. *Proc. Natl. Acad. Sci. U.S.A.* **2002**, *99*, 10982−10987.
(41) Beljonne, D.; Cornil, J.; Silbey, R.; Millié, P.; Brédas, J. L. Interchain interactions in conjugated materials: The exciton model versus the supermolecular approach. *J. Chem. Phys.* **2000**, *112*, 4749−4758.
(42) Spano, F. C. Modeling disorder in polymer aggregates: The optical spectroscopy of regioregular poly(3-hexylthiophene) thin films. *J. Chem. Phys.* **2005**, *122*, 234701.
(43) Chang, J. F.; Clark, J.; Zhao, N.; Sirringhaus, H.; Breiby, D. W.; Andreasen, J. W.; Nielsen, M. M.; Giles, M.; Heeney, M.; McCulloch, I. Molecular-weight dependence of interchain polaron delocalization and exciton bandwidth in high-mobility conjugated polymers. *Phys. Rev. B* **2006**, *74*, 115318.
(44) Spano, F. C.; Clark, J.; Silva, C.; Friend, R. H. Determining exciton coherence from the photoluminescence spectral line shape in poly(3-hexylthiophene) thin films. *J. Chem. Phys.* **2009**, *130*, 074904.
(45) Westenhoff, S.; Daniel, C.; Friend, R. H.; Silva, C.; Sundstrom, V.; Yartsev, A. Exciton migration in a polythiophene: Probing the spatial and energy domain by line-dipole Forster-type energy transfer. *J. Chem. Phys.* **2005**, *122*, 094903.
(46) Scheblykin, I. G.; Yartsev, A.; Pullerits, T.; Gulbinas, V.; Sundstrom, V. Excited state and charge photogeneration dynamics in conjugated polymers. *J. Phys. Chem. B* **2007**, *111*, 6303−6321.
(47) Mikhnenko, O. V.; Cordella, F.; Sieval, A. B.; Hummelen, J. C.; Blom, P. W. M.; Loi, M. A. Temperature dependence of exciton diffusion in conjugated polymers. *J. Phys. Chem. B* **2008**, *112*, 11601−11604.
(48) Athanasopoulos, S.; Emelianova, E. V.; Walker, A. B.; Beljonne, D. Exciton diffusion in energetically disordered organic materials. *Phys. Rev. B* **2009**, *80*, 195209.